

Microphotoluminescence studies of single quantum dots. II. Magnetic-field experiments

U. Bockelmann, W. Heller, and G. Abstreiter

Walter Schottky Institut, Technische Universität München, Am Coulombwall, D-85748 Garching, Germany

(Received 13 May 1996)

We perform microphotoluminescence measurements on a series of single GaAs/Al_xGa_{1-x}As quantum dots of various lateral confinement in magnetic fields up to 5 T. A diamagnetic shift and a Zeemann spin splitting of the luminescence lines depending on the size of the structure is observed. The characteristic diamagnetic shift demonstrates the excitonic origin of the luminescence. The spin splitting increases with the exciton energy. [S0163-1829(97)06807-0]

In recent years, there has been a lot of work on the interband optical properties of low-dimensional semiconductor systems in magnetic field.¹⁻¹¹ The application of a magnetic field to a quantum dot leads to a diamagnetic shift and a Zeemann spin splitting of the energy levels. The excitonic states are characterized by three energy scales: the lateral size quantization energy $\hbar\omega_0$, the exciton effective Rydberg energy $\mu e^4/(\epsilon^2\hbar^2)$, and the magnetic confinement energy $\hbar\omega_c$. When the lateral quantization and the Coulomb attraction are increased by decreasing the lateral dot size, the magnetic confinement becomes less important, leading to a decreasing diamagnetic shift. On the other hand, when the magnetic field dominates, we approach the limit of two-dimensional magneto-excitons.

In this paper we present magnetic-field studies on a series of quantum dots which was produced by laser-induced thermal interdiffusion of a GaAs/Al_xGa_{1-x}As quantum well.¹² This method allows us to vary the lateral structure size systematically. Using a microphotoluminescence (μ -PL) setup we perform spectroscopy on a single quantum dot at a time. In contrast to measurements on dot arrays, inhomogeneous line broadening is avoided.

The experimental setup is shown schematically in Fig. 1. The PL is excited by an Ar⁺ laser beam (514 nm) which is focused by a microscope objective into the cryostat to a spot size of about 1.5 μ m at the sample surface. The sample is mounted in a specially designed continuous flow cryostat (Oxford Instruments) which contains a superconducting magnet, and provides magnetic fields up to 5 T. The sample is at a temperature of 4 K. With an XYZ translation stage we move the laser spot relative to the sample, which allows us to address the desired single quantum dot. The PL signal is analyzed by a triple Raman spectrometer with multichannel detection. The detection area (about 2 μ m in diameter) is defined by a pinhole which is placed at an image plane. We detect the circular polarization of the luminescence with a quarter-wave plate in front of the spectrometer.

In the following we present experimental results of quantum-dot structures with a lateral geometrical size w of 1 μ m, 500 nm, 450 nm, and 400 nm. The appropriate measure of the strength of the lateral confinement is the line splitting in the μ -PL spectrum, and not simply the size w . The maximum line splitting of about 10 meV is observed for an intermediate value of $w = 450$ nm. See Sec. II of part I (previous paper¹³) and Ref. 12 for a description of the investigated

quantum-dot series. The 1- μ m dot essentially behaves like a bidimensional system. The lateral confinement is very weak, and there is only a single luminescence line which exhibits no significant shift with respect to the PL of the as-grown quantum well. Application of a constant magnetic field along the growth direction leads to a blueshift of the PL line as presented in Fig. 2. At a maximum field of 5 T the luminescence line is shifted by about 1.1 meV. As we will see now, the electron-hole Coulomb interaction has to be considered to explain this small value.

The wave function for the lateral relative coordinate $\vec{r} = \vec{r}_e - \vec{r}_h$ of the quantum-dot exciton is described by the two-dimensional effective-mass Hamiltonian

$$H_{\text{rel}} = \frac{\vec{p}^2}{2\mu} + \frac{1}{2}\mu\omega^2 r^2 - \frac{e^2}{\epsilon r}, \quad (1)$$

with the reduced mass $\mu = m_e^* m_h^* / (m_e^* + m_h^*)$, $\omega_c = eB/2\mu$, and $\omega = \sqrt{\omega_0^2 + \omega_c^2}$. ω_0 defines the strength of the parabolic lateral confinement. Assuming the same ω_0 for the electron and hole, the relative and the center-of-mass motions are decoupled, and the whole magnetic-field dependence of the problem is contained in the Hamiltonian H_{rel} .^{8,9} Discarding excitonic effects by neglecting the last term on the right side of Eq. (1), for the magnetic-field dependence of the ground-state energy we obtain

$$E_0 = \hbar\omega = \hbar\sqrt{\omega_0^2 + \omega_c^2}. \quad (2)$$

For very weak lateral confinement, we can neglect ω_0 and obtain a linear magnetic-field dependence $E_0 = \hbar\omega_c$ which corresponds to a slope of about 1.4 meV/T in GaAs with $\mu = 0.042m_0$. At $B = 5$ T we thus obtain a shift of 6.9 meV which is much higher than the experimental result. We can, however, describe the experimental findings if we take the electron-hole Coulomb interaction into account. In a regime where the Coulomb interaction is much stronger than the lateral confinement one can use the wave functions of the two-dimensional hydrogenic problem (H_{rel} with $\omega = 0$) and treat the lateral potential to first order of perturbation theory. This approach is well justified for the 1- μ m structure, where the lateral confinement is very small compared to the exciton binding energy. For the ground state energy, we obtain

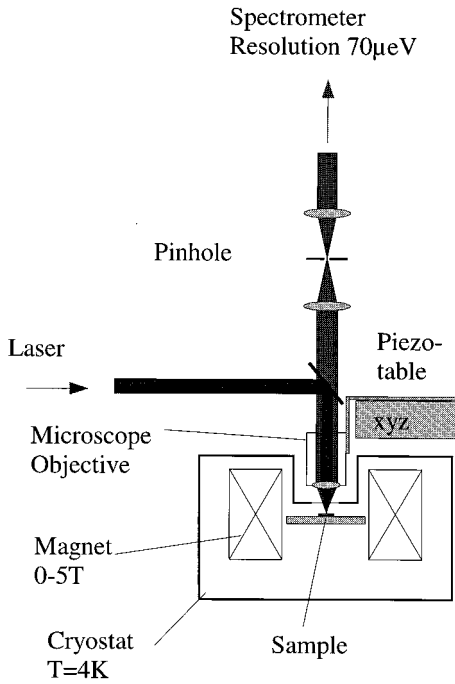


FIG. 1. Schematic view of the experiment.

$$\langle 0|H_{\text{rel}}|0\rangle = -2 \frac{\mu e^4}{\epsilon^2 \hbar^2} + \frac{3}{16} \frac{\epsilon^2 \hbar^4}{\mu e^4} \omega^2. \quad (3)$$

In the present perturbation treatment, the resulting quadratic diamagnetic shift Δ of the ground-state energy is independent of the confinement parameter ω_0 .

$$\Delta = \langle 0|H_{\text{rel}}|0\rangle_B - \langle 0|H_{\text{rel}}|0\rangle_{B=0} = \frac{3\epsilon^2 \hbar^4}{16\mu e^4} \omega_c^2 \quad (4)$$

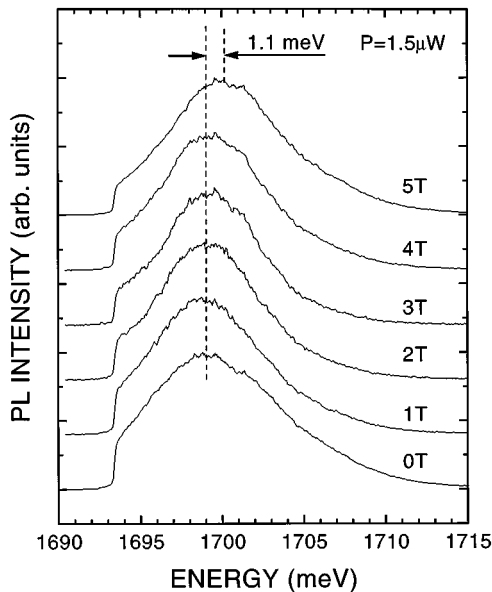


FIG. 2. Dependence of the peak energy of the 1- μm sample on the magnetic field. The lower limit of the detection window is observable at 1693 meV.

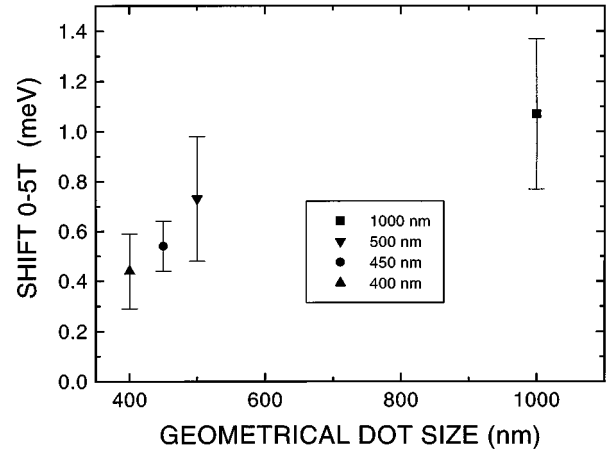


FIG. 3. Dependence of the diamagnetic shift on the lateral dot size w .

For the heavy hole exciton in GaAs ($\epsilon/4\pi\epsilon_0=13$), we obtain $\Delta=1.3$ meV at $B=5$ T. The exciton binding energy given by the first term on the right of Eq. (3) is 13.5 meV. The shift of 1.1 meV observed on the 1- μm dot fits quite well with the estimated value of Δ . To explain the small measured shifts without excitonic effects, we would have to set the lateral confinement parameter $\hbar\omega_0$ to unreasonably high values above 20 meV. We can therefore conclude that our μ -PL spectra are of excitonic origin.

Figure 3 shows the measured magnetic-field shift of the ground-state energy as a function of the geometrical dot size w . There is a systematic decrease of the shift with decreasing w . With increasing lateral confinement the magnetic field becomes less important, leading to a weaker shift of the luminescence line. Reducing w below about 450 nm in our structures, we do not observe a further increase, but a reduction of the lateral confinement accompanied by an increasing blue-shift of the whole spectrum.¹² Supported by model calculations of the local laser-induced intermixing, this indicates the beginning of sizable alloying close to the dot center. The corresponding higher effective mass of the exciton state should result in an increase of the binding energy. The magnetic confinement therefore becomes less important compared to the exciton binding which results in a reduced diamagnetic shift. This effect might explain why we do not observe a stronger magnetic-field dependence on the 400-nm dot than on the 450-nm dot, although the lateral confinement, deduced from the μ -PL line splitting, is smaller for $w=400$ nm.

Figure 4 shows a series of spectra of the 450-nm dot at 0 and 5 T for various excitation intensities. The strong luminescence from the higher-energy levels has been attributed to a slowing down of energy relaxation induced by the complete spatial quantization.¹² We see that with increasing excitation power the luminescence from the second peak grows relative to the ground state. This change indicates an additional reduction of the relaxation induced by a filling of the ground state. It gives further support to one central result of the time-resolved measurements, namely, that in the quantum-dot structures the exciton seems to obey the Pauli exclusion principle.^{13,14}

It was theoretically predicted that a magnetic field leads to

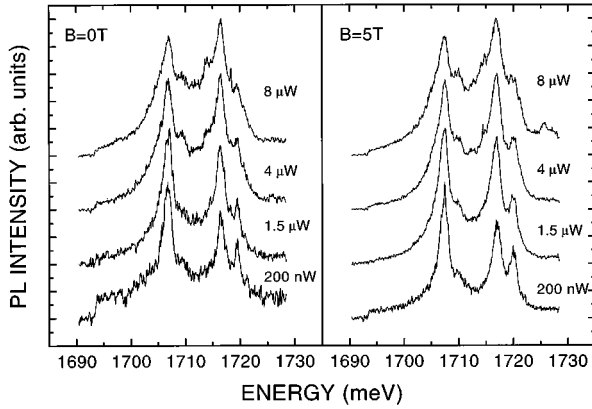


FIG. 4. PL spectra of the $w=450$ nm quantum dot for $B=0$ and 5 T at various excitation powers.

an enhanced exciton relaxation within the dot, and that the excited-state luminescence should be reduced accordingly.⁹ Figure 5 shows numerical computations on the intensities of the lowest three radiative transitions for a parabolic quantum dot at zero temperature. Details of the rate-equation analysis are given in Ref. 15. From this calculation we indeed expect the intensity ratio of the lowest 2 peaks to change by about a factor of two when the magnetic field, is applied. Experimentally, the PL intensity of the whole spectrum increases with magnetic field, but a systematic change in the relative intensities is not observed. This result holds down to very weak excitation intensities where we estimate less than one exciton in the dot on the time average (see part I, Sec. V B). The discrepancy indicates that the actual confinement potential deviates from the parabolic shape used in the calculation. The calculations also predict a different magnetic-field dependence for the individual lines of the $w=450$ nm dot (see Ref. 9, Fig. 6) which is not observed either.

At $B=5$ T, we measure a Zeemann spin splitting with a quarter-wave plate in front of the spectrometer. This way we can resolve a splitting of about 0.5 meV, as shown in Fig. 6,

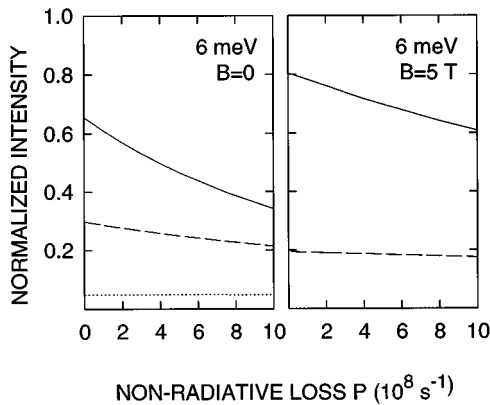


FIG. 5. Calculated PL intensities from the ground state and the first and second excited radiative excitons of the $w=450$ nm structure (solid, dashed and dotted lines, respectively) for $B=0$ and 5 T. A rate equation based on calculated radiative lifetimes and LA-phonon-scattering times of the lowest exciton states is solved numerically. A single phenomenological loss rate P is assumed for all states to describe nonradiative recombination. State-filling effects are not included. For $B=5$ T the dotted line is very close to zero.

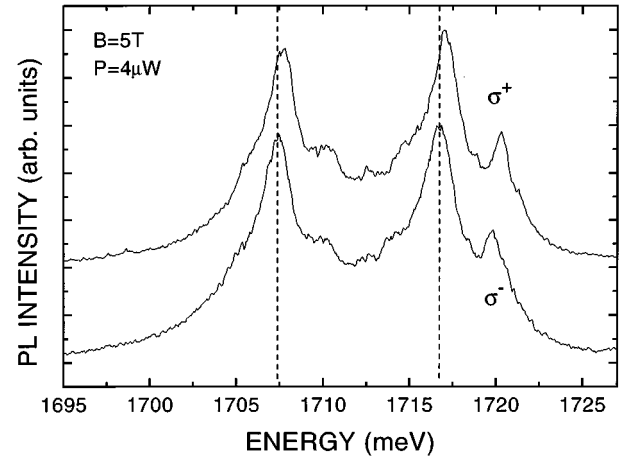


FIG. 6. PL spectra of the 450 -nm structure with σ^+ and σ^- circularly polarized detection. Excitation is provided without circular polarization.

while without circularly polarized detection we only see a slightly broadened line (see Fig. 4). Figure 7 shows that the splitting increases with increasing peak energy. In the following we briefly discuss the possible origin of this energy dependence.

In a magnetic field the electron and hole states split up according to spin. Only transitions between electron and hole states which change the spin by a value of ± 1 are optically allowed. For the heavy-hole exciton emission this means that there are two PL lines with opposite circular polarizations. The energy difference between the spin-split states is described by $\Delta E_e = g_e^* \mu_B B$ for the electron and $\Delta E_h = g_h^* \mu_B B$ for the heavy hole. $\mu_B = e\hbar/(2m_0)$ is the Bohr magneton, m_0 is the free-electron mass, and g_e^* and g_h^* are the effective g factors of the electron and hole. It was experimentally observed that in quantum wells the electron g factor g_e^* depends on the well width, and even a reversal of the sign of g_e^* was found at a well width of about 5 nm.¹⁶ The electron g factor for bulk GaAs is $g_e^* = -0.44$. In the case of $\text{Al}_x\text{Ga}_{1-x}\text{As}$, g_e^* increases with x , becomes positive at $x=0.12$, and reaches $g_e^* = 0.5$ for the $\text{Al}_{0.35}\text{Ga}_{0.65}\text{As}$ barrier of our as-grown quantum-well structure.¹⁷ In a rough picture the increase of g_e^* with the well width can thus be

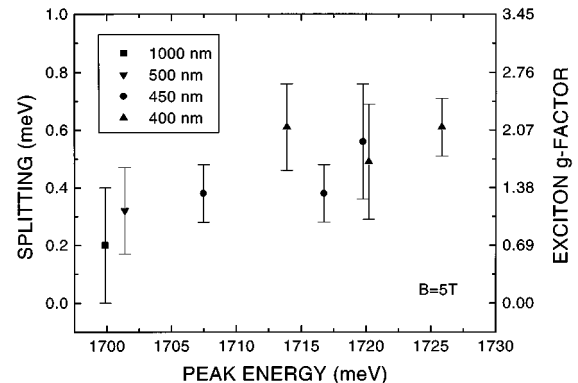


FIG. 7. Dependence of the Zeemann spin splitting (left) and the exciton g factor (right) on the energy of the PL line for several single dot structures.

attributed to the increasing leakage of the wave function into the barrier. The quantitative theoretical description given by Ivchenko and Kizelev¹⁷ emphasizes the importance of the electron energy and band nonparabolicity. Comparison of measured electron and exciton g factors leads to the conclusion, that the spin-splitting of an exciton line, described by the exciton g factor $g^* = g_e^* + g_h^*$, is dominated by the Zeeman splitting in the valence band.⁶ A strong increase of the g factor g^* with decreasing well width has been observed for quantum-well excitons.^{6,18} The reduction of the well width corresponds to an increasing quantization energy. Therefore an increase of g^* with the PL energy might also be expected for quantum dots. Our experimental result, presented in Fig. 7, shows such a dependence. To our knowledge there exists neither a theory for the well-width dependence of the exciton g^* in quantum wells, nor any

theoretical work on the spin splitting of quantum-dot excitons.

In summary, we have reported on microphotoluminescence experiments on single artificial quantum dots in magnetic fields. We have observed a diamagnetic shift which depends systematically on the lateral confinement. We have not seen enhanced exciton relaxation predicted theoretically for quantum-dot excitons in magnetic field. The size of the measured Zeemann spin splitting increases with the energy of the corresponding PL line, which in turn is a function of the dot size.

We thank K. Brunner, G. Böhm, and G. Weimann for providing the samples, and M. Bichler for his contributions to the cryostat design. The work was supported financially by the Deutsche Forschungsgemeinschaft (SFB 348) and the Bundesministerium für Bildung und Forschung (III-V Nanoelektronik Verbundprojekt).

-
- ¹J. C. Maan, G. Belle, A. Fasolino, M. Altarelli, and K. Ploog, *Phys. Rev. B* **30**, 2253 (1984).
²W. Ossau, B. Jäckel, E. Bangert, G. Landwehr, and G. Weimann, *Surf. Sci.* **174**, 188 (1986).
³G. E. W. Bauer and T. Ando, *Phys. Rev. B* **37**, 3130 (1988).
⁴L. Viña, G. E. W. Bauer, M. Potemski, J. C. Maan, E. E. Mendez, and W. I. Wang, *Phys. Rev. B* **41**, 10 767 (1990).
⁵J. B. Stark, W. H. Knox, D. S. Chemla, W. Schäfer, S. Schmitt-Rink, and C. Stafford, *Phys. Rev. Lett.* **65**, 3033 (1990).
⁶M. J. Snelling, E. Blackwood, C. J. McDonagh, R. T. Harley, and C. T. B. Foxon, *Phys. Rev. B* **45**, 3922 (1992).
⁷U. Bockelmann and G. Bastard, *Phys. Rev. B* **45**, 1700 (1992).
⁸V. Halonen, Tapash Chakraborty, and P. Pietiläinen, *Phys. Rev. B* **45**, 5980 (1992).
⁹U. Bockelmann, *Phys. Rev. B* **50**, 17271 (1994).
¹⁰A. Zrenner, L. V. Butov, M. Hagn, G. Abstreiter, G. Böhm, and G. Weimann, *Phys. Rev. Lett.* **72**, 3382 (1994).
¹¹M. Bayer, A. Schmidt, A. Forchel, F. Faller, T. L. Reinecke, P. A. Knipp, A. A. Dremin, and V. D. Kulakovskii, *Phys. Rev. Lett.* **74**, 3439 (1995).
¹²K. Brunner, U. Bockelmann, G. Abstreiter, M. Walther, G. Böhm, G. Tränkle, and G. Weimann, *Phys. Rev. Lett.* **69**, 3216 (1992).
¹³U. Bockelmann, W. Heller, A. Filoramo, and Ph. Roussignol, preceding paper, *Phys. Rev. B* **55**, 4456 (1997).
¹⁴U. Bockelmann, Ph. Roussignol, A. Filoramo, W. Heller, G. Abstreiter, K. Brunner, G. Böhm, and G. Weimann, *Phys. Rev. Lett.* **76**, 3622 (1996).
¹⁵U. Bockelmann, *Phys. Rev. B* **48**, 17 637 (1993).
¹⁶M. J. Snelling, G. P. Flinn, A. S. Plaut, R. T. Harley, A. C. Tropper, R. Eccleston, and C. C. Phillips, *Phys. Rev. B* **44**, 11 345 (1991).
¹⁷E. L. Ivchenko and A. A. Kiselev, *Fiz. Tekh. Poloprovodn.* **26**, 1471 (1992) [*Sov. Phys. Semicond.* **26**, 827 (1992)].
¹⁸R. M. Hannak, M. Oestreich, A. P. Heberle, and W. W. Rühle, *Solid State Commun.* **93**, 313 (1995).